

GEOLOGICAL MAPPING IN THE CHELEKEN PENINSULA, TURKMENISTAN AREA USING ADVANCED SPACEBORNE THERMAL EMISSION AND REFLECTION RADIOMETER (ASTER) DATA

P. Junek ^{a,b}

^a CTU Prague, Faculty of Civil Engineering, Dept. of Mapping and Cartography, Thakurova 7, 16629 Prague 6, Czech Rep.
junek@gama.fsv.cvut.cz

11/2002 – 9/2003 an exchange student at:

^b Delft University of Technology, Faculty of Civil Engineering and Geosciences, Dept. of Applied Earth Sciences, Mijnbouwstraat 120, 2628 RX Delft, Netherlands

PS WG IV/7

KEY WORDS: Remote Sensing, Geology, Mapping, Multispectral, Analysis

ABSTRACT:

High number of geological phenomena – outcropping Pliocene rocks (Red Series), former and recent mud volcanoes, hydrothermal brines rich in Pb and Zn – which can provide significant information to understand sedimentology of South Caspian Basin (SCB) can be found on the Cheleken Peninsula, Turkmenistan. To test ability of ASTER imagery for mapping of these phenomena and their comparison with other areas located in SCB region was the aim of this research.

For this purpose ASTER Surface Reflectance data (AST_07) were processed. In the first stage all remotely sensed data were geometrically pre-processed (so as to have the same geodetic reference). In the second stage, the different false color composite images and image enhancement techniques were applied to the data and geological photo interpretation was carried out. In the third stage, different band ratio techniques were applied to the data and in the fourth stage, the spectral mapping technique (Matched Filtering) in order to map different mineral groups were accomplished.

The photo interpretation of enhanced imagery (saturation stretched ASTER 631 bands shows the best results) was useful to obtain basic knowledge of the area and localize main geological phenomena mentioned in literature. Band rationing (ASTER1 / ASTER2) is powerful tool for mapping the Red Series outcrops due its significantly higher values of ratio than other rocks of the Cheleken Peninsula. Different mineral groups (such as AL-OH bearing minerals – Alunite + Phryphyllite group, Kaolinite group, Muscovite + Illite group; Carbonates + Mg-OH bearing minerals) were mapped using band rationing and Matched Filtering.

ASTER imagery allowed us to carry out preliminary geological investigation of the area and find encouraging research methods in terms of mapping the main geological phenomena occurring around the peninsula. The results are not confirmed by field spectra or other additional data.

1. INTRODUCTION

1.1 Aim of Study

The Earth Science Group of Delft University of Technology is involved in research in the Caspian area since 1991. The main goal is to collect data on the impact of sea-level change on sedimentary sequences in different time scales and to develop simulation models of fluvial and near shore sedimentary systems. To that end several projects have been carried out in the Volga and Kura delta. These projects have improved understanding of reservoir architecture in these areas.

A third important South Caspian Basin delta system is in Turkmenistan. Outcropping Paleo-Amudarya Sediments form the backbone of Cheleken Peninsula in Turkmenistan. This Peninsula is not only the site of onshore and offshore oil production, but also produces hydrothermal brines rich in Pb and Zn, in a comparable way as mud volcanoes in Azerbaijan. In contrast to the modern Volga and Kura deltas, the modern Amu Darya (or Uzboy) delta is not functioning any more as a delta, as the river has been diverted towards the Aral Sea in historic times. Therefore, this abandoned delta is virtually devoid of vegetation. This opens a possibility for direct spaceborne mapping and spectral comparison with other deltas around the region.

1.2 Geologic Setting of Cheleken Peninsula

Cheleken Peninsula (53°15' E, 30°28' N) is located on the east bank of Caspian Sea in Turkmenistan (Central Asia) (*fig. 1*).

Cheleken Peninsula lies on the Absheron-Balkhan sill, which divides South Caspian Basin from North Caspian Basin. Jackson, 2002 discusses in detail active tectonics of South Caspian Basin and conducts the fact that SCB stands as an aseismic block about 300x300 km large surrounded by belts of intense earthquake activity, where Absheron-Balkhan sill is one of those belts. The major fold evolution in the Cheleken Peninsula area affecting the Pliocene Red Series and younger sediments causes the right-lateral strike-slip motion between SCB and Euroasia (NCB). As a result of this movement process several anticlines have been formed in the east part of SCB where the backbone of Cheleken Peninsula (Chochrak Ridge) is one of anticline axes and represents outcrop of Pliocene Red Series onto the surface.

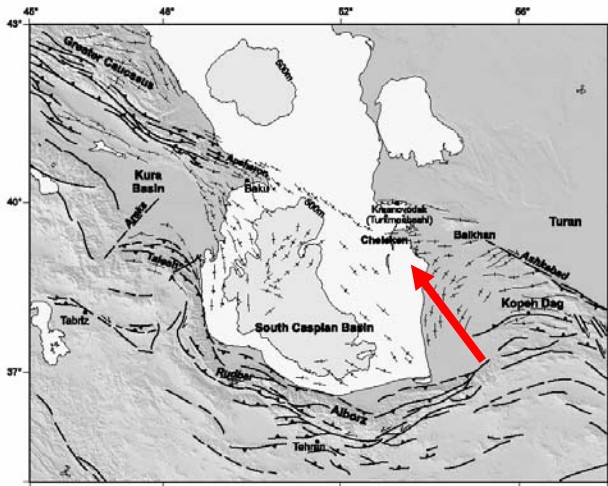


Figure 1. Summary structural map of the South Caspian Basin, Jackson et al., 2002.

Central morphological element of the peninsula is Chochrak Ridge, which reaches 92 metres above sea level (119 metres above Caspian Sea level) and is ranged from NE to SW. The ridge is formed by Middle and Upper Pliocene series – “Red Series” – nowadays crossed by hundreds of deep erosion gullies, some of those drain brines out of sand-argillaceous Pliocene beds (Dvorov, 1975). Lower Pliocene layers do not achieve the surface and thus can not be studied using remote sensing. The rest of peninsula is formed of Quarternary sediments of Akchagyl, Absheron, Baku, Khazar and Chvalin stages (fig.2).

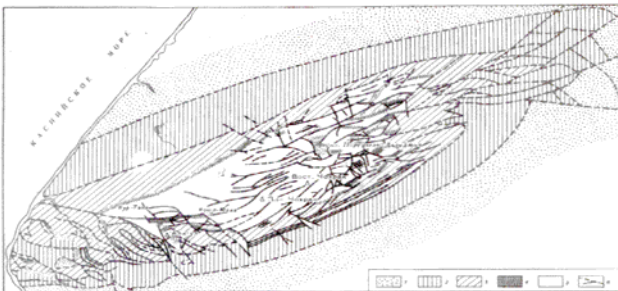


Figure 2. Geological schema of Cheleken (according to A.S.Arhipthenko,1956); red series (white area in the centre) are surrounded by other beds.

Chochrak Ridge is semicircular surrounded by solonchaks – small muddy areas, which especially southwards acquires the largest size. Solonchaks are formed as a result of extensive brines activity linked with faulting of Pliocene rocks and with erosion of Chochrak Ridge. These processes allow brines reach the surface and thus change the surface rocks.

The other phenomenon linked with faulting is presence of mud volcanism. Three volcanoes of different age occurs in the area: remains of Upper Pliocene or Post-Pliocene mud volcano Aligul are situated on the SE slope of Chochrak, in the western part of the peninsula, approximately 2 kilometres of Caspian shoreline, is situated active mud volcano of Zapadnyj Porsugel. Its mud-flows are discharged south and northwards of the crater. In the NE of Chochrak can be found lake of Rozovyj Porsugel – former mud volcano crater flooded by water.

During Post-Pliocene times have been formed numerous marine-built terraces, which describe sea-levels of Chvalinsk

Sea. Second and third Chvalinsk terrace is sloped to NNW due to Post-Chvalinsk uplift of Cheleken anticline formation.

1.3 ASTER instrument

The ASTER sensor was launched in December 1999 on board the Earth Observation System (EOS) US Terra satellite to record solar radiation in 14 spectral bands (fig. 3.). ASTER measures reflected radiation in three bands between 0.52 and 0.86 μm (Visible and Near Infrared - VNIR) and in six bands from 1.6 to 2.43 μm (Shortwave Infrared - SWIR), with 15-metres spatial resolution. Furthermore, ASTER also has a back-looking VNIR telescope with 15-m resolution. Thus, stereoscopic VNIR images can be acquired at 15-m resolution. In addition, emitted radiation measured at 90-m resolution in five bands in the 8.125-11.65 μm wavelength region (Thermal Infrared - TIR). The swath width is 60 km, but ASTER’s pointing capability extends the total cross-track viewing capability to 232 km. A very important aspect of the EOS Program is the open availability of the data from all the instruments including on-demand standard products in the low costs. ASTER standard products include VNIR and SWIR surface radiance and reflectance, brightness temperature at the sensor, TIR surface radiance and emissivity, surface kinetic temperature, decorrelation-stretch images and digital-elevation models (DEM).

Jet Propulsion Laboratory of NASA has already in 1995 carried out the prospective capability of ASTER sensor using simulated data from AVIRIS airborne sensor [2]. Conclusions of the study has shown that VNIR data are sensitive to the presence of iron oxide minerals; the SWIR data highlight the presence and differences of minerals with hydroxyl radicals and carbonates, such as clays, alunite, and limestone; the TIR data are sensitive to differences in silica-bearing rocks, either in the presence of or in the absence of the other mineral constituents.

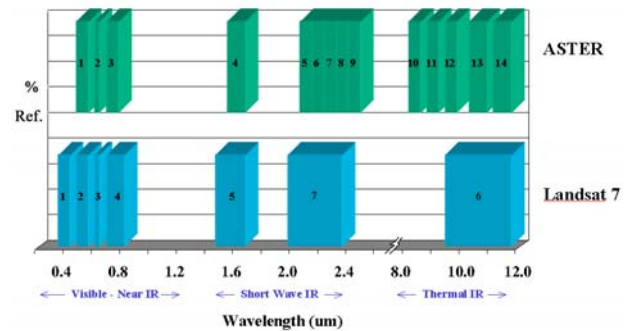


Figure 3. Comparison of ASTER and LANDSAT ETM+ spectral resolution.

Several studies have been published during 2001 (Hewson, 2001) respectively 2003 (Rowan, 2003) on ASTER data evaluation in test sites. Both studies compare precisely geological mapped (by field survey and airborne hyperspectral or multispectral sensors as AVIRIS, AMS-HyMap, Hyperion etc.) areas to test ability of use of ASTER imagery.

2. CONCEPTION AND METHODOLOGY

2.1 Used Data

We have used on-demand product ASTER Surface Reflectance (AST_07) from the EROS Data Center (EDC), which contains surface reflectance for each of the nine VNIR and SWIR bands at 15-m and 30-m resolutions, respectively. The results are obtained by applying an atmospheric correction to radiances reported by the ASTER sensor. The atmospheric correction removes effects due to changes in satellite-sun geometry and atmospheric conditions. The atmospheric correction algorithm is applied to clear-sky pixels only and the results are reported as a number between 0 and 1 (Abrams, ASTER User Handbook). As additional information for support the ASTER Digital Elevation Model has been used.

2.2 Workflow of Study

The processing of ASTER Surface Reflectance data (AST_07) consists of four steps. In the first stage all remotely sensed data were geometrically pre-processed (so as to have the same geodetic reference). In the second stage, the different false color composite images and image enhancement techniques were applied to the data and geological photo interpretation was carried out. In the third stage, different band ratio techniques were applied to the data and finally, in the fourth stage, the spectral mapping techniques (as Matched Filtering, ENVI software technique and Variable Multiple Spectral Mixture Analysis, García-Haro – 2001) in order to map different mineral groups were accomplished.

However Russian authors discuss in detail geochemical characteristics, the information about geospatial distribution of phenomena is insufficient and can be just supposed (no geographic information as maps or coordinates is mentioned). This fact does not allow us to get precise knowledge of the area and thus to link spatially maps in Dvorov, 1975 or Lebedev, 1983 with satellite imagery.

2.3 Image Interpretation

Different band combinations have been tested to provide best image interpretation using false-colour composite image. Other RS techniques (contrast stretches, histogram equalization, image transformations) was applied for image enhancement before interpretation.

Following false-colour composite images has been used to carry out interpretation of study area:

- *321 false-colour composite* to obtain the best spatial resolution images and to get basic information about vegetation across the area
- *631 false-colour composite* has showed the most clear differences in the geological and geographical information mentioned in the literature

Bands 321 false-colour composite is commonly used in order to highlight the presence of vegetation, which appears in red shades whereas the other land cover types are decreased. In the ASTER imagery can be used 321 bands instead of Landsat 432 bands. The whole area is shown in brown shades except the small areas close to settlements (Cheleken City and unknown village) which are most likely irrigated gardens. The rest of peninsula should be avoid of vegetation or sparsely covered.

Bands 631 false-colour composite has proven to be the most worthwhile for mapping of geological phenomena. Roughly, the

area is divided into three parts. The north part represents flat plain covered by eolic sand covers (dunes) appearing light yellow or red-brown, the central part (*fig. 4*) is formed by various types of phenomena – Red Series – shown in light yellow and highly disrupted by system of erosion gullies; mud volcanoes shown in pink colour (situated in the neighbourhood of Red Series – Aligul respectively Rozovyy Porsugel, and in the W part of image (Zapadnyj Porsugel); solonchaks are situated mostly along fault on the SE slope of Chochrak Ridge and between Aligul and Zapadnyj Porsugel or as a result of recent volcanic activity of Zapadnyj Porsugel mud volcano. The brines affected areas appears from dark green to dark brown shades. Man affected areas NW from Chochrak, which surrounds rectangular reservoirs and appear in dark grey or black. The south part represents flat plain gently sloped towards South Cheleken Bay. Most of the area appears in light blue, cyan or white colours, in some areas disrupted by solonchaks (dark green shades).

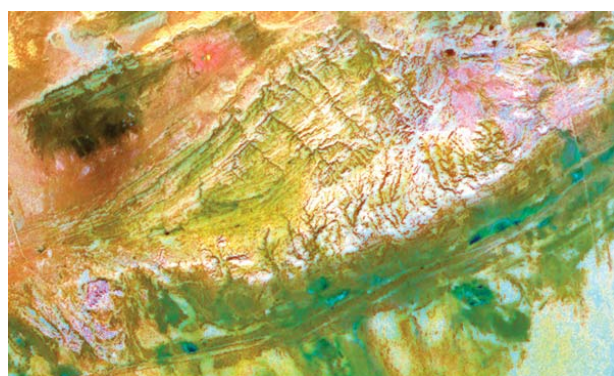


Figure 4. Bands 631 colour composite approved best capability to map geological phenomena across whole peninsula. Red series appear as triangle in the centre, mud volcano deposits appear as pink areas westwards (Aligul) and eastwards (Rozovyy Porsugel) from Red series.

2.4 Band Rationing

Ratio images designed to display the spectral contrast of specific absorption features have been used extensively in geologic remote sensing and vegetation mapping.

ASTER band 1 / band 2 ratio image. Ratio of these wavelengths has been successfully used by Segal, 1989, who have used Landsat TM bands 3/2 ratio to map iron-bearing rocks in Lisbon Valley, Utah. According to Hunt, 1977, ferric-iron (Fe^{3+}) rich rocks exhibit a sharp fall-off in reflectance approximately from 0.8 micrometers to shorter wavelengths, thus ferric-iron rich exposures exhibit very low ASTER band 1/ band 2 values.

When band rationing has been applied to Cheleken data, the lowest band ratio values clearly represent Red Series situated in the middle of the scene and confirms supposition, that red-colouring of beds is caused by higher iron content of rock layers. Besides the Red Series, low ratio values appear in some areas of the North Plain located most likely at summits of sand dunes, which are one of landscape-forming feature mentioned by Dvorov, 1975.

The newest studies of geochemical characteristics of Holocene sediments in the Aral Sea region have found out significant difference between Syr Darya and Amu Darya sediments. The

Syr Darya deposits are enriched in gypsum, aragonite and calcite. Diatoms are hardly observed. On the contrary, the Amu Darya sediments are characterized by aragonite and Mg-calcite precipitation and high Fe and Mn carbonate contents (Le Callonnec).

If the geochemical characteristics of Amu Daria sediments have not changed from Pliocene to Holocene era, then is reasonable to expect high Fe contents in Red Series of Cheleken Peninsula, which are formed by Pliocene-aged Paleo Amu Darya sediments.

The use of ASTER band 1 / band 2 can be affected by band 2 (660 nm) absorption feature which is caused most likely by chlorophyll and other pigments contained in green vegetation (Mather, 1999). This fact has been ignored in this study, because the vegetation mapping based on NDVI has shown no or sparse vegetation cover in the areas which in spite of it shows band 2 absorption feature (presence of chlorophyll). The spatial distribution of band 2 absorption is not linked with NDVI values and band 2 / band 1 ratio values. In other words, if exists any sparse vegetation cover (exhibited by band 2 absorption), it should not affect the conclusion that Red Series can be mapped by ASTER band 1/ band 2 ratio. This problem can be solved by purchasing other VNIR data of the study area (as Landsat ETM+ or SPOT), which can give additional information.

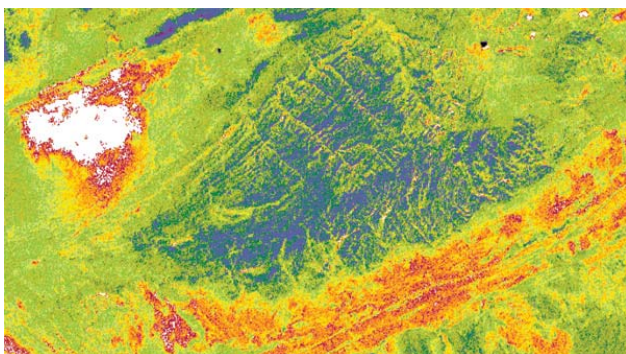


Figure 5. ASTER band 1/ band 2 ratio image shows ability to map outcrops of Red series, which have the lowest values of ratio in the area (the lowest values appear in blue, the highest appear red), compare with Figure 4.

ASTER SWIR band rationing to map major mineral groups. Ratio images designed to display the spectral contrast of specific absorption features have been used extensively in geologic remote sensing and Rowan, 2003 has already applied this remote sensing technique on ASTER data to carry out lithologic mapping in the Mountain Pass, California area. Relative absorption depth (RBD) images are an especially useful three-point ratio formulation for displaying Al-O-H, Mg-O-H and CaCO₃ absorption intensities prior to conducting more detailed, time-consuming spectral analysis. For each absorption feature, the numerator is the sum of the bands representing the shoulders (bands 1 and 2), and the denominator is the band located nearest the absorption feature minimum (band 3); removal of continuum increases the intensity of the absorption feature:

$$\text{RBD} = (\text{band 1} + \text{band 2}) / \text{band 3} \quad (1)$$

Several different RBD images have been created. The ((band 7 + band 9)/band 8) RBD image which highlights the CaCO₃ and

Mg-O-H absorption feature at 2237.5 nm is affected by higher values of band 9 caused by ASTER SWIR instrument problem (Scholte, 2003), thus the presence of absorption feature occurs across whole studied area, with exception of pixels located along NW coast, where sharp fall-off of spectra from band 8 towards band 9 overestimate the higher values of band 9.

In order to eliminate the effect of band 9, the threshold value has been changed to get more presumable result. First is possible to state, the presence of absorption feature is linked with brine activity, the other areas which most likely contain CaCO₃ bearing minerals are roads in Cheleken City and on some other places of peninsula. The presence of the band 8 absorption feature differ two areas classified as dunes. Whereas the bright dunes (G) show absorption feature at 2237.5 nm (even without correction of band 9), the dunes close to the north sand bar has some absorption at this wavelength. These dunes have other spectral characteristic then other dunes in the area (more Calcite like then Alunite).

The Al-O-H absorption RBD image ((band 5 + band 7)/band 6) shows that this absorption feature is in general distributed in areas of brines activity, but highly significant is that brines in NE part of Chochrak Ridge does not show presence of Al-O-H groups (and thus can be easily differentiated from the other brines). As other meaningful fact appears that large areas in the SE part of the scene shows presence of Al-O-H Mica absorption as well, but more detailed look at the spectra shows that these areas have broad absorption feature both in Al-O-H Mica and Al-O-H Phyrrophyllite group. The presence of Al-O-H Mica absorption feature could be caused by stronger brine activity in the past.

The largest areas are covered by Al-O-H Alunite & Phyrrophyllite absorption RBD image which occurs on most areas. Generally the pixels belong either to Al-O-H Alunite or to Al-O-H Mica group.

The ((band 5 + band 9)/band 8) RBD image successfully maps distribution of pixels dominated by deep absorption at 2237.5 nm, which are linked with brine activity located in NE part of Cheleken. The spectra of other brine ponds mapped by this band ratio show both dominating 2237.5 nm absorption and less distinct absorption feature caused by Al-O-H Mica group.



Figure 6. ASTER SWIR band ratio highlighting strong absorption feature at 2237.5 nm (probably carbonates and Mg-O-H group).

2.5 Spectral methods

Spectral signatures of minerals in SWIR. Several spectra of minerals from USGS Spectral library have been resampled to demonstrate major spectral signatures of minerals in SWIR. Minerals characterized by absorption feature near 2165 nm

belong to group of AIOH bearing minerals e.g. Pyrophyllite and Alunite. Jarosite represents sulphite minerals and has absorption feature at 2260 nm. Minerals with absorption feature near 2327.5 nm belongs either to CaCO₃ or MgOH bearing minerals – this group of minerals represent Calcite, Chlorite or Talc. Group of minerals which has absorption feature near 2205 nm is represented by Montmorillonite, Kaolinite, Muscovite or Illite. Whilst will be not possible to map particular minerals using ASTER imagery, it will be possible to differentiate between mentioned mineral groups.

Selection of endmembers. Selecting of different types of endmembers which represent spectrally most extreme pixels in the scene has been provided by support of pixel purity index technique (PPI). PPI is a means of finding the most “spectrally pure” pixels typically correspond to mixing endmembers. The PPI is computed by repeatedly projecting n-dimensional scatterplots onto a random unit vector. The extreme pixels in each projection are recorded and the total number of times each pixel is marked as extreme is noted (ENVI User’s Guide). The spectra with specific spectral characteristics or of areas important for geological setting has been also studied, but have not been noted as extreme and are not used for spectral analyses. The image scene has been divided into several areas according to conclusions of image interpretation and has been focused to map geological and geographical phenomena occurring on peninsula.

Matched filtering is an ENVI software technique which performs partial unmixing – finding the abundances of user defined endmembers. Not all of the endmembers in the image need to be known. This technique maximizes the response of the known endmember and suppresses the response of the composite unknown background, thus “matching” the known signature. It provides a rapid means detecting specific materials based on matches to library or image endmember spectra and does not require knowledge of all endmembers within an image scene (ENVI User’s Guide). Bands 4-9 have been processed by Matched Filtering in order to map area according to its SWIR spectral signatures. Following spectra have been collected:

- a/ WpoolW – which represents the pixels with 2205 nm absorption, no pixels with absorption at 2205 and without absorption at 2237.5 nm at the same time have been found in the image scene.
- b/ Solonchak – represents pixel with deepest absorption feature at 2165 nm
- c/ Dunes bright – represents pixels with absorption at 2165 nm and with no absorption at 2237.5 nm
- d/ Top of duine – represents pixels with absorption at 2165 nm and 2237.5 nm
- e/ NE pool – represents pixels with deep absorption at 2237.5 nm

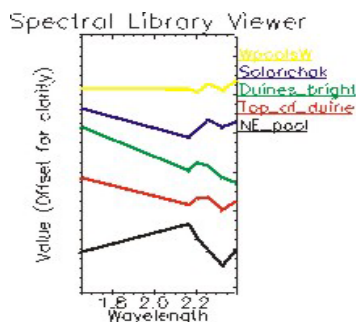


Figure 7. Spectra of selected endmembers in the SWIR.

The study area has been successfully mapped using matched filtering procedure. Results of matched filtering are shown as three endmembers colour composite (in red, green respectively blue colour) where higher matches are represented by brighter pixels. Figure 8 shows western part of Red Series outcrops where pixels with different spectral signatures are mapped. The randomly collected spectra of bright pixels demonstrate that technique is able to classify image according to spectra signatures (plot).

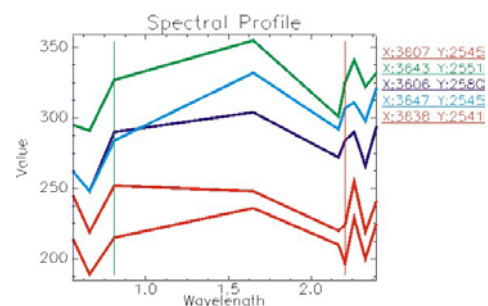
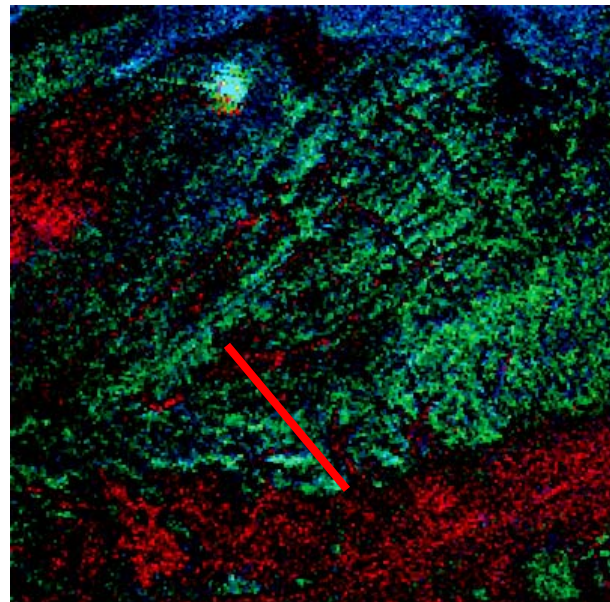


Figure 8. The matched filtered image of west part of Red Series shows different spectral signatures along the profile (red line). Red pixels (both in image and plot) have absorption feature at 2205 nm and 2237.5 nm, green and blue have absorption both 2165 nm and 2237.5 nm, when green one have deeper the first absorption feature and blue ones the later.

3. CONCLUSIONS

Analysis of ASTER spectral reflectance data of Cheleken Peninsula provides promising results. ASTER imagery allowed us to carry out preliminary geological investigation of the area and find encouraging research methods in terms of mapping the main geological phenomena occurring around the peninsula. False-color composite images are useful to get an overview about the area and map different types of rocks and land covers. Band rationing is a mean to map Red Series (ASTER band 1/ band 2) and distribution of hydroxyl and carbonates bearing minerals. Thanks to Matched Filtering technique surprising facts have been discovered – two types of areas influenced by

brine activity and bedding like distribution of pixels in the west part of Red Series outcrops.

The results are not confirmed by field spectra or other additional data. It is important to notice that previously published scientific papers about ASTER data use data only together with further information (field data, airborne hyperspectral data – e.g. AVIRIS).

In the further research could be helpful to make comparison of ASTER imagery with other satellite or airborne data (Landsat, SPOT, aerial photographs) – especially to make clear the band 2 absorption feature (more in chapter Band rationing).

ACKNOWLEDGEMENT

This research has been carried out during stay of author at the Earth Science Group of Delft University of Technology, The Netherlands from 11/2002 to 9/2003. His stay has been supported by Socrates/ERASMUS scholarship. The processed data were used by the courtesy of the Ministry of Agriculture and the research part was processed within the GA CR project 205/03/0218 research and Vyzkumny zamer 210000007. Poster presentation in the frame of XXth ISPRS Congress has been supported by Interni grant CVUT – 84037-11153.

REFERENCES

Mather, P.M., 1999. *Computer Processing of Remotely-Sensed Images*. John Wiley & Sons, pp. 292

Abrams, M., Hook S.J., 1995. Simulated Aster Data for Geologic Studies. *IEEE Transactions on Geoscience and Remote Sensing*, Vol. 33, No. 3

Segal, D.B., Merin, I.S., 1989. Successful Use of Landsat Thematic Mapper Data for Mapping Hydrocarbon Microseepage-Induced Mineralogic Alteration, Lisbon Valley, Utah. *Photogrammetric Engineering and Remote Sensing*, Vol. 55, No. 8, pp. 1137-1145

Hunt, G.R., 1977. Spectral Signatures of Particulate Minerals in the Visible and Near Infrared. *Geophysics*. Vol. 42, No. 3, pp501-513

Dvorov, V.I., 1975. *Termalnyje vody Chelekena (in Russian)*, Izdatelstvo “Nauka”, Moskva

Le Callonnec, L. et.al – Geochemical Changes of the Aral Sea Water during the Regressive Events from the Last 11000 Years *EUG Symposium Holocene Paleoclimate Records over Europe and the North-Atlantic* (abstract)

Rowan, L.C., Mars, J.C., 2003. Lithologic mapping in the Mountain Pass, California area using Advanced Spaceborne Thermal Emission and Reflection Radiometer (ASTER) data *Remote sensing of Environment*, 84, pp.350 – 366

ENVI User's Guide, Research Systems, Inc., 1999

Jackson, J., Priestley, K., Allen, M., Berberian, M., 2002. Active tectonics of the South Caspian Basin. *Geophys. J. Int.* 148, 214-245

Abrams, M., Hook, S., XXXX. *ASTER User Handbook - Version 2*, NASA Jet Propulsion Laboratory, California, USA.

Hewson, R.D., Cudahy, T.J., Huntington, J.F., 2001. Geologic and alteration mapping at Mt Fitton, South Australia, using ASTER satellite-borne data, *IEEE*, 2001, pp.724-726

Lebedev, L.M., Nikitina, I.B., 1983. *Chelekenskaja rudoobrazujusaja sistema* (in Russian). Izdatelstvo “Nauka”, Moskva.

Hornibrook, M. Spectral unmixing of ASTER data, Escondia North, Chile, Geoimage PTY Ltd.

Scholte, K.H., Hommels A., van der Meer, F.D., Kroonenberg, S.B., Hanssen, R.F., Aliyeva, E., Huseynov, D., Guliev, I., Preliminary ASTER and InSAR Imagery Combination for Mud Volcano Dynamics, Azerbaijan.

http://www.itc.nl/library/Papers_2003/peer_ref_conf/vandermeer.pdf (Accessed on 23 April 2004)